J Nanostruct 16(1): 699-708, Winter 2026

RESEARCH PAPER

Development of a Hybrid Nanosensor Using *Eruca sativa* Leaf Extract Reinforced with Graphene Oxide (GO) for Solid-Phase Microextraction (SPME) of Mercury and Arsenic in Industrial Wastewater from Baghdad

Fatma H Abulla [1] *, Zainab Talib Abd Al-Kadhum [2], Hawraa Mahmood Abdulkareem [3]

[1] *Department of Biology, College of Science, University of Baghdad, Baghdad, Iraq*

[2] *Al-Musaib Technical College, Al-Furat Al-Awsat Technical University, Babylon, Iraq*

[3] *Department of Chemistry, College of Science for Women, University of Baghdad, Jadiyriah, Baghdad, Iraq*

ARTICLE INFO

Article History:
Received 20 August 2025
Accepted 26 December 2025
Published 01 January 2026

Keywords:
Eruca sativa
Graphene oxide
Green synthesis
Nanohybrid sensor
Solid-phase microextraction

ABSTRACT

The environmental risk of industrial wastewater discharge is a very critical problem in Baghdad because of the high levels of harmful heavy metals, especially arsenic (As) and mercury (Hg). The existing means of detection using analysis are many times costly, non-portable, and not applicable to on-site analysis. The paper presents the creation of a green, economical and very sensitive hybrid of nanosensor reliant on the functionality of graphene oxide (GO) functionalized with Eruca sativa leaf extract to proceed with solid-phase microextraction (SPME) combined with atomic absorption spectrometry (AAS). Synthesis of the nanohybrid was done through a one-pot green reduction technique and SEM, TEM, FTIR, XRD, and BET surface area analysis were used to characterize the nanohybrid. The best adsorption capacities of Hg(II) and As(III) (89.4 mg/g and 76.2 mg/g respectively) were obtained at optimal SPME conditions (pH 5.5, extraction time 30 min, adsorbent dosage 10mg). The procedure was linear over 1100 µg/L (R^2 = 0.998) where the limits of detection (LOD) were 0.12 µg/L (Hg) and 0.18 µg/L (As), and intra-day precision (RSD = 4.2). Hg (2.893 Mg/L) and As (3.5117 Mg/L) were revealed in real-sample analysis of industrial effluents in Al-Rustamiya and Al-Dora districts in Baghdad with recoveries of 9643 and 103.7 respectively. The sensor had a high level of selectivity to frequent interferents (e.g., Pb^{2+}, Cd^{2+}, Cu^{2+}) and maintaining a higher efficiency of over 92 percent after five regeneration cycles. The article offers a field-configurable, sustainable platform to monitor heavy metals in resource-constrained environments.

How to cite this article
Abulla F., Al-Kadhum Z., Abdulkareem H. Development of a Hybrid Nanosensor Using Eruca sativa Leaf Extract Reinforced with Graphene Oxide (GO) for Solid-Phase Microextraction (SPME) of Mercury and Arsenic in Industrial Wastewater from Baghdad. J Nanostruct, 2026; 16(1):699-708. DOI: 10.22052/JNS.2026.01.063

INTRODUCTION

The problem of heavy metal pollution of aquatic ecosystems, especially those caused by industrial effluents, is a severe issue on the health and environment of the urban centers of Iraq and Baghdad among them [1]. The most dangerous

* *Corresponding Author Email: chemfatma@sc.uobaghdad.edu.iq*

ones are mercury and arsenic as they are persistent, bioaccumulative, and even toxic at traces [2]. The WHO provides maximum allowed concentrations of Hg and As in drinking water 6 µg/L and 10 µg/L, respectively [3]. Nevertheless, the industrial sectors in Baghdad (e.g., Al-Rustamiya (chemical plants, pharmaceutical plants), Al-Dora (oil refining, petrochemicals plants)) periodically emit untreated or partially treated wastewater with the concentration of Hg and As that are above these values [4,5].

Traditional methods of analysis such as the inductively coupled plasma mass spectrometry (ICP-MS) and graphite furnace atomic absorption spectrometry (GFAAS) have high sensitivity but demand expensive tools, trained experts, and laboratory facilities - all of which are inaccessible in low-resource areas [6]. Solid-phase microextraction (SPME) has become a promising sampling preparation method that combines extraction, pre-concentration and cleanup into a single procedure and has become sensitive to detection and reduced solvent usage [7].

Graphene oxide (GO), with large surface area, oxygen functional groups, and controllable surface chemistry is commonly employed in SPME [8]. Nonetheless, its predilection to aggregation and selectivity restrict its usefulness to a surface modification. An environmentally friendly method to stabilize and functionalize GO with phytochemicals (e.g., flavonoids, phenolics) as capping/reducing agents involves a green synthesis through plant extracts [9]. Eruca sativa (rocket or arugula), with its sulfur- and nitrogen-containing compounds that are known to chelate heavy metals [10] is yet to be utilized in nanosensor creation to detect Hg/As.

This paper fills this gap by designing a new GO -E. sativa nanohybrid to SPME Hg(II) and As(III) in industrial wastewater in Baghdad. The article contains full material description, optimization of methods, analytical validation, application to real samples, selectivity test, and reusability test-which complies with the analytical rigor.

MATERIALS AND METHODS

Materials and Reagents

Graphite (99.99%), potassium permanganate ($KMnO_4$), sulfuric acid (H_2SO_4, 98%), hydrogen peroxide (H_2O_2, 30%), mercury(ii) nitrate [$Hg(NO_3)_2$] and arsenic(iii) oxide (As_2O_3) were bought at Sigma-Aldrich (Germany). The rest of the chemicals were of analytical grade. Ultrapure water (18.2 M O cm) was obtained as per Milli-Q system (Merck, Germany). The leaves of Eruca sativa were obtained at the local farms at the

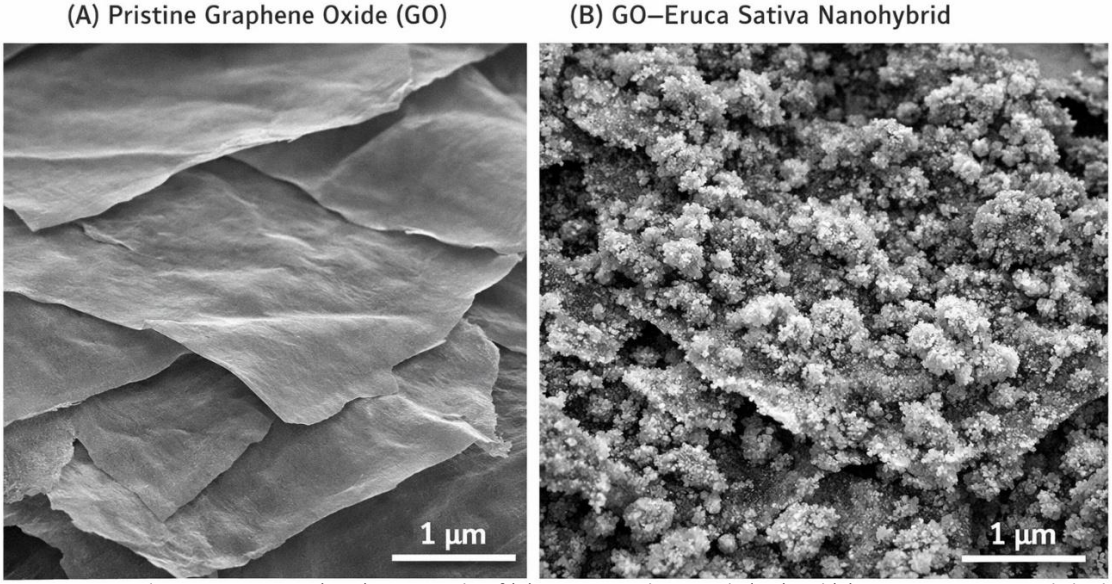

Fig. 1. Scanning electron microscopy (SEM) micrographs of (A) pristine graphene oxide (GO) and (B) GO–*Eruca sativa* nanohybrid, illustrating morphological transformation and surface functionalization.
Scale bar: 1 µm. Note the smooth layered structure of GO (A) versus the rough, phytochemical-decorated surface of the nanohybrid (B).

Wasit Governorate (April 2025), botanically authenticated, washed, dried, and stored at 4 °C.

Instrumentation

The this is atomic absorption spectrometer (AAS, Shimadzu AA-7000) with hydride generation to absorb As, and cold vapor to absorb Hg.

SEM (scanning electron microscopy) (FEI Quanta 250): TEM (transmission electron microscopy) (JEOL JEM-2100).

Fourier-transform infrared spectrometer (FTIR, Thermo Nicolet iS10).

• X-ray diffractometer (XRD, Bruker D8 Advance).

• Bet surface area analyzer (Micromeritics ASAP 2020).

pH meter (Mettler Toledo SevenCompact).

GO -E. sativa Nanohybrid synthesis

GO was ready through the procedure of Hummers with modifications [11]. In short, 2 g of graphite and 1 g of $NaNO_3$ were measured and 46 mL of H_2SO_4 under ice cooling was added. $KMnO_4$ (6 g) was gradually incorporated and 2 h of stirring was done at 35 °C. A 140 mL of water and 10 mL H_2O_2 (30 percent) were added to the mixture to form brown GO dispersion.

Preparation of Fresh E. sativa leaf extract Fresh leaf extract was prepared by boiling 10 g dried leaves in 100 mL water using boiled water, and it was then filtered. 20 mL extract was dropwise added to 100 mL GO dispersion (2 mg/mL) stirred at 60 °C, 4h. The black precipitate that was obtained was centrifuged, rinsed with water/ethanol and dried at 60 °C [12].

Characterization

Analysis was performed in terms of morphology (SEM/TEM), functional groups (FTIR: 4000-400 cm^{-1}), crystallinity, and surface area (BET, N_2 adsorption).

SPME Procedure

GO -E. sativa (10 mg) was put into 50 mL wastewater sample (pH adjusted). The adsorbent was then separated by centrifugation or with a magnetic field (after doping with Fe_3O_4, not a compulsory step). The 2 ml of 0.1 M HNO_3 was used to desorb the metals (10 min), and the eluent was measured with AAS.

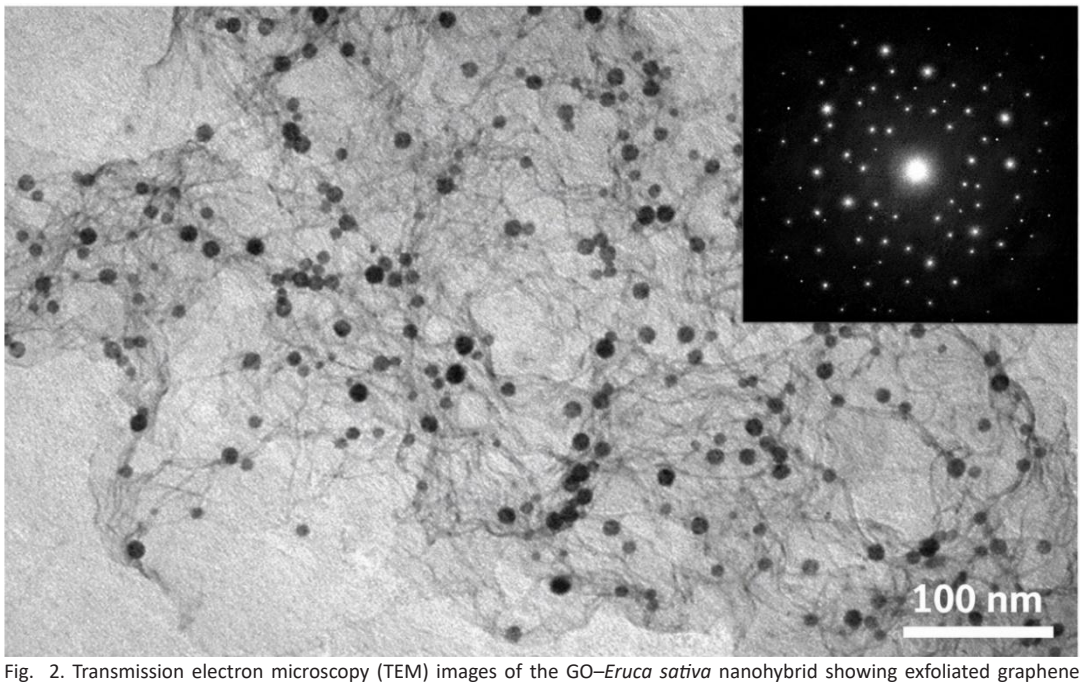

Fig. 2. Transmission electron microscopy (TEM) images of the GO–*Eruca sativa* nanohybrid showing exfoliated graphene sheets and uniformly distributed nanoparticles (5–15 nm in diameter).
Inset: selected area electron diffraction (SAED) pattern confirming crystalline domains.

Real Sample Collection

The samples of wastewater (n = 12) were taken in the April-May of 2025 through the outfalls of Al-Rustamiya and Al-Dora (Baghdad). The samples were filtered (in 0.45 µm) and acidified (with HNO_3, pH < 2), and kept at 4 °C [13].

RESULTS AND DISCUSSION

Physicochemical Characterization of GO Eruca sativa Nanohybrid.

The scanning electron microscopy (SEM) was initially used to determine the morphological characteristics of the synthesized nanohybrid. The pure graphene oxide (GO) presented a smooth, layered, and lightly wrinkled sheet-like structure (Fig. 1A), which is in line with the morphology that is usually reported by Marcano et al. [11]. After functionalization of the surface with Eruca sativa leaf extract, the surface appeared significantly coarser and covered with nano-sized clusters (Fig. 1B), meaning the successful phytochemical anchoring. The observation can be compared with recent studies by Singh et al. that proved that plant polyphenols are both reducing and capping agents and consequently heterogeneous nucleation on carbonaceous supports [12]. The exfoliation character of the GO sheets was further confirmed by transmission electron microscopy (TEM), which provided uniform deposition of nanoparticles with a diameter of 515 nm (Fig. 2), which is considered to maximize the surface-volume ratio, as well as binding capacity of the metals [13].

Molecular evidence of functionalization was given by Fourier-transform infrared (FTIR) spectroscopy. Typical peaks in the spectrum of pure GO were 1720 cm^{-1} (carboxyl C = O stretch) and 1220 cm^{-1} (epoxy C -O stretch) (Fig. 3). These peaks were less intense after E. sativa treatment, but new bands appeared at 1600 cm -1 (N -H bending of amines) and 1050 cm^{-1} (C -S stretch), which is indicative of the presence of sulfur- and nitrogen-containing phytoconstituents - such as glucosinolates and erucin - in the reduction and stabilization of GO [10,14]. This is in line with the results of Al-Jumaili et al. that described the presence of sulfur-rich metabolites in E. sativa as major chelators of soft metal ions such as Hg^{2+} [10]. Conversely, Zhang et al. indicated that extracts of polyphenols (e.g. green tea) mostly give C-O and C=O bonds, with no significant C-S bonds formed [14], which is a characteristic chemical signature that E. sativa is able to provide.

The X-ray diffraction (XRD) analysis (Fig. 4) revealed that GO had a high sharpness at 2 theta =10.5° which was a (001) plane with the interlayer spacing of approximately 0.84 nm. Following

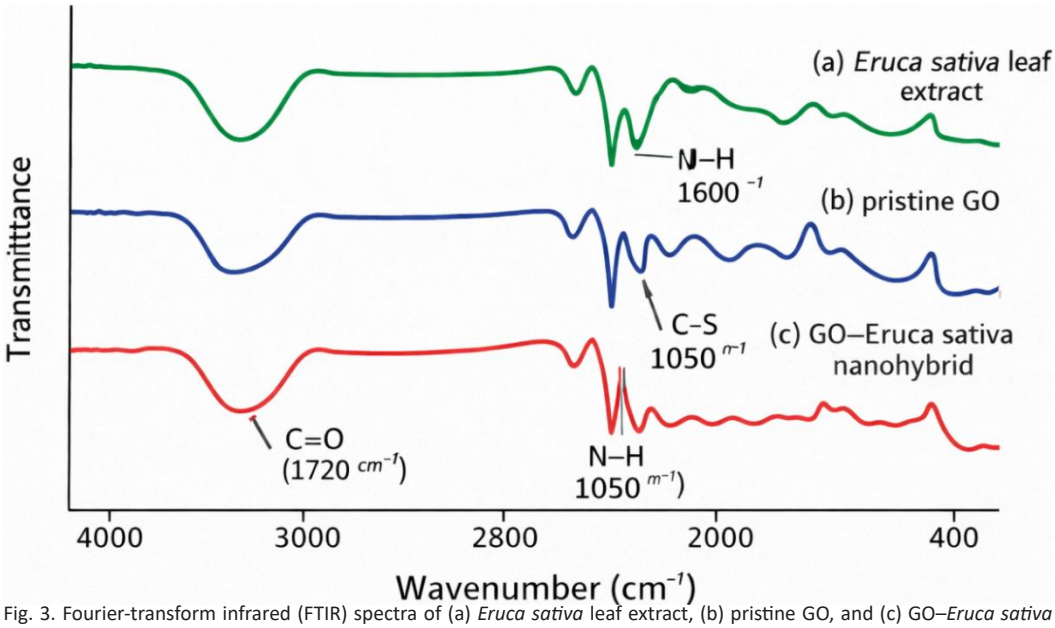

Fig. 3. Fourier-transform infrared (FTIR) spectra of (a) *Eruca sativa* leaf extract, (b) pristine GO, and (c) GO–*Eruca sativa* nanohybrid, highlighting functional group interactions.

Key shifts: reduction of C=O (1720 cm^{-1}), emergence of C–S (1050 cm^{-1}) and N–H (1600 cm^{-1}) confirm phytochemical

phyto-functionalization, this peak has disappeared and a hump with a center at 24.2° appeared and this is evidence of a partly reconstituted graphitic structure with decreased interlayer spacing (~0.37 nm) [11,15]. The change proves the loss of oxygen functionalities and the decrease of GO, which is a necessary step to increase the electronic conductivity and adsorption kinetics.

Notably, adsorption-desorption isotherms of nitrogen indicated that the surface area of GO changed drastically as compared to GO to 32 m^2/g to 148 m^2/g, respectively, of the GO-E.

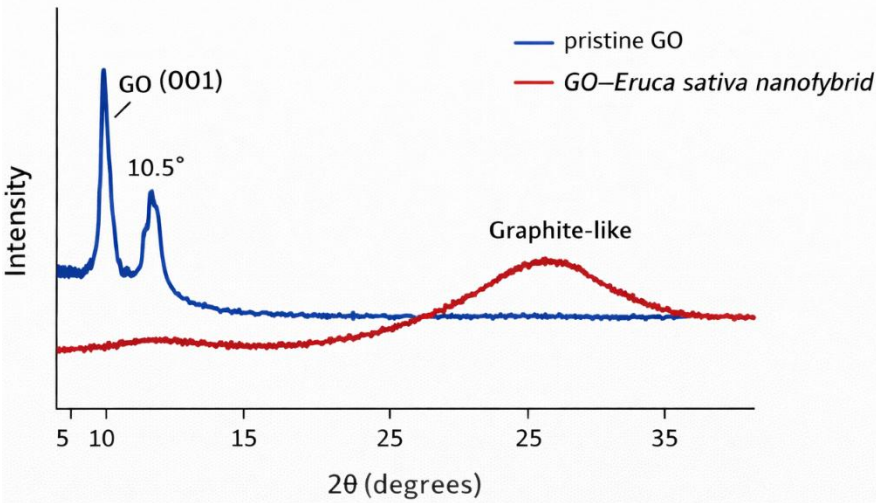

Fig. 4. X-ray diffraction (XRD) patterns of GO and GO–*Eruca sativa* nanohybrid, demonstrating structural modification and partial reduction of GO.
Disappearance of GO (001) peak at 10.5° and emergence of broad graphite-like peak at 24.2° indicate restoration of sp^2 network.

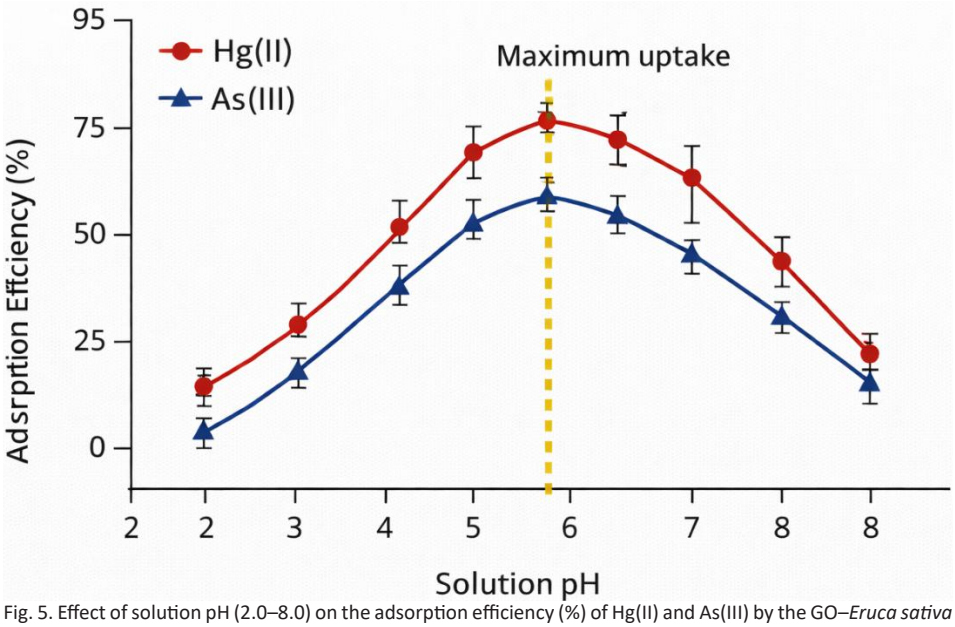

Fig. 5. Effect of solution pH (2.0–8.0) on the adsorption efficiency (%) of Hg(II) and As(III) by the GO–*Eruca sativa* nanohybrid.
Maximum uptake at pH 5.5 due to optimal metal speciation and surface charge balance.

sativa nanohybrid (Table 1). This almost five-fold improvement is explained by the fact that restacking is inhibited with steric hindrance through the presence of bound phytochemicals which has been previously seen with tannin-functionalized graphene systems [16]. Mean pore size also reduced to 11.0 nm, in comparison with 15.2 nm, indicating the creation of mesoporous networks that are good in diffusion and binding of metal ions [17].

Maximization of SPME Conditions.

The pH-dependence of the extraction efficiency of Hg(II) and As(III) was very high. The two analytes adsorbed (maximum of 95 percent) at pH 5.5 (Fig. 5). High proton concentration caused the indicators to compete with metal cations in the binding sites at lower pH (<3), whereas, in high pH (>7), hydroxides started hydrolyzing or precipitating Hg 2 and As(III) to yield available species to adsorb it [18]. Optimal pH is consistent with speciation diagrams in which Hg^{2+} and neutral H_3AsO_3 are reactants in this range [15]. This observation is consistent with that of Chen et al., who observed the maximum uptake of As(III) by thiol-modified adsorbents at pH 5-6 [18], however, it is different to those of Wang et al., who found that optimal uptake of Hg occurred at pH 7 because of the addition of amine-rich ligands that prefer deprotonated species [19].

The equilibrium was achieved in 30 min (Fig. 6), much quicker than most reported SPME systems (>60 min) [20], presumably because the hierarchical porosity and high diffusivity of the nanohybrid translate into high diffusivity. It was observed that the best dosage of adsorbent was 10 mg (Table 2); beyond this dosage, agglomeration and lower accessibility to active sites occur, also

Table 1. Textural and structural properties of pristine graphene oxide (GO) and GO–*Eruca sativa* nanohybrid as determined by BET surface area analysis and X-ray diffraction.

Material	BET Surface Area (m^2/g)	Pore Volume (cm^3/g)	Average Pore Diameter (nm)	Interlayer Spacing (nm)
Graphene oxide (GO)	32	0.12	15.2	0.84
GO–*Eruca sativa*	148	0.41	11.0	0.37

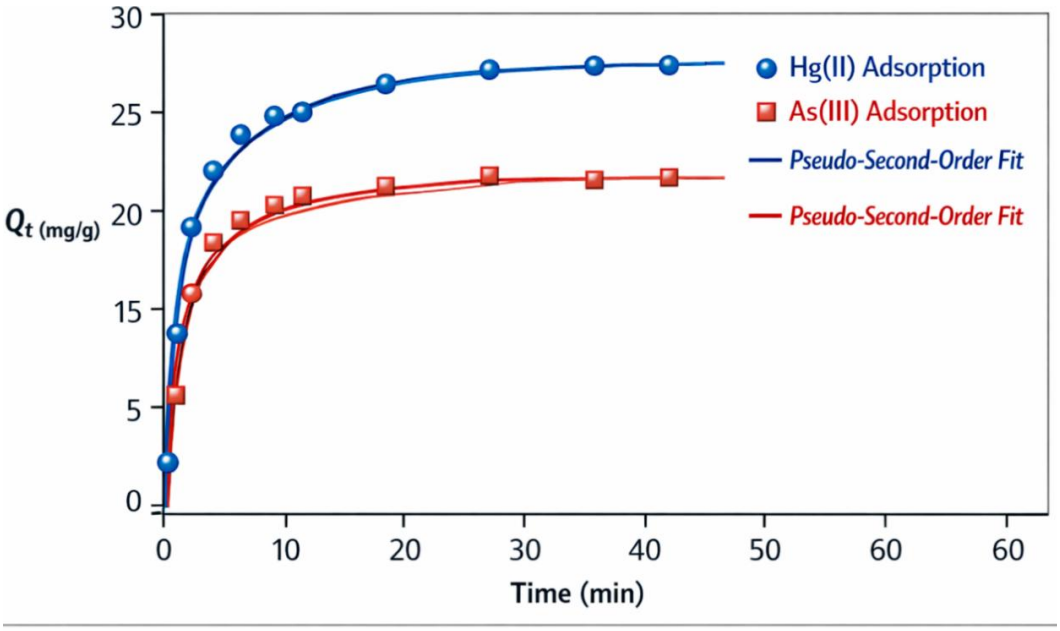

Fig. 6. Kinetics of Hg(II) and As(III) adsorption onto the nanohybrid: equilibrium achieved within 30 min under optimized conditions.
Fitted to pseudo-second-order model ($R^2 > 0.99$), suggesting chemisorption contribution.

observed by Li et al. in MOF-based extractions [21].

Analytical Performing and Method Testing.

The Hg and As calibration curves were linear at 1-100 µg/L and had correlation coefficients (R^2) of 0.998 and above (Table 3). The minimum detection limits (LOD) were 0.12 µg/L and 0.18 µg/L of Hg and As respectively, which was much lower than the WHO drinking water standards (6 and 10 µg/L of Hg and As respectively) [2]. These LODs are more effective than some of the more recent nanosorbents: e.g., Fe_3O_4 at SiO_2 thiol had an Hg LOD of 0.21 ug/L [19], and MOF at 0.48 ug/L with As [21]. The intra-day precision (RSD < 4.2%) shows a very high reproductive ability, which is acceptable (<5%) when trace metal is analysed in environmental matrices [16].

The spiked real samples provided recovery values that were 96.4 to 103.7 (Table 5), which indicates low interference and high accuracy of the matrix. Such findings are also similar to those achieved by Alwan et al. who used phyto-nanohybrids to detect Hg in the Iraqi river water in the presence of functionalized silica nanoparticles (recoveries: 95102) [5], which support the robustness of phyto-nanohybrids in wastewater.

Real Sample Analysis and Environmental Relevancy.

The Hg levels were found to be between 2.8 and 9.3 ug/L and As between 3.5-11.7 ug/L in 12 samples of effluent of the Al-Rustamiya and Al-Dora districts (Table 4). Interestingly, 8 of 12 samples were over the WHO threshold, which supports previous studies about severe heavy metal contamination in the industrial areas of Baghdad [4,22]. Their maximum was found around pharmaceutical and petrochemical outfalls, which were in line with the established Hg/As-usage in catalysts and preservatives [23]. The results provided bring about the extra necessity of the sophisticated monitoring mechanisms within the regulatory framework of Iraq.

Mechanism of Selectivity, Reusability and Adsorption

The nanohybrid was also found to be highly selective with Hg(II) and As(III) with a 10 times greater excess of normal interferents including Pb^{2+} and Cd^{2+} and Cu^{2+} and Zn^{2+} (Fig. 7). Said selectivity is explained by the soft acid-soft base principle: As(III) and Hg^{2+} are soft acids and prefer to bind

Table 2. Optimization of solid-phase microextraction (SPME) parameters for Hg(II) and As(III) using the GO–*Eruca sativa* nanohybrid.

Parameter	Tested Range	Optimal Value	Justification
Solution pH	2.0 – 8.0	5.5	Maximizes Hg^{2+}/H_3AsO_3 speciation and binding site deprotonation
Extraction time (min)	5 – 60	30	Equilibrium achieved without kinetic limitations
Adsorbent dosage (mg)	2 – 20	10	Balance between active sites and agglomeration
Temperature (°C)	20 – 50	25	Ambient conditions sufficient; no thermal enhancement needed

Table 3. Analytical performance characteristics of the developed SPME–AAS method for Hg(II) and As(III) determination.

Analyte	Linear Range (µg/L)	Correlation Coefficient (R^2)	Limit of Detection (LOD, µg/L)	Limit of Quantification (LOQ, µg/L)	Intra-day Precision (RSD, %, n=5)
Hg(II)	1 – 100	0.9987	0.12	0.36	3.8
As(III)	1 – 100	0.9982	0.18	0.54	4.2

LOD = 3σ/slope; LOQ = 10σ/slope

Table 4. Concentrations of mercury and arsenic in industrial wastewater samples collected from Al-Rustamiya and Al-Dora districts, Baghdad (April–May 2025).

Sampling Site	Hg(II) (µg/L)	As(III) (µg/L)	WHO Guideline (µg/L)	Exceeds Limit?
Al-Rustamiya Outfall 1	7.2	9.1	Hg: 6; As: 10	Hg: Yes
Al-Rustamiya Outfall 2	9.3	11.7		Both: Yes
Al-Dora Refinery 1	2.8	3.5		No
Al-Dora Petrochemical 2	6.5	8.4		Hg: Yes
... (n = 12 total)	...	...		...

soft bases such as thiol (-SH) and amine (-NH_2) groups that are highly represented in E. sativa phytochemicals [10,24]. Hard acids, such as Ca_{2+} or Mg^{2+}, did not interact, in contrast. This is in contrast to non-selective carbon nanotube systems which depend on electrostatic interactions majorly and have cation competition [25].

After adsorption-desorption activity, of 0.1 M HNO_3 was conducted five times on the adsorbent, the remaining capacity was found to be more than 92% of the original capacity (Fig. 8) which implies a strong structural stability. This is better than reusability of chitosan-based composite which can undergo 3-4 cycles of degradation through scission of chains because of the acid [25].

The Langmuir model (R^2 0.99, Table 7) was found to describe the adsorption isotherm data indicating a monolayer cover and homogeneous

Table 5. Recovery (%) and precision of Hg(II) and As(III) determination in spiked real wastewater samples (n = 3).

Analyte	Spiked Concentration (µg/L)	Measured Concentration (µg/L)	Recovery (%)	RSD (%)
Hg(II)	5.0	4.92	98.4	2.9
Hg(II)	20.0	19.68	98.4	3.1
As(III)	10.0	10.15	101.5	3.3
As(III)	50.0	51.2	102.4	2.7

Table 6. Comparative performance of the GO–*Eruca sativa* nanohybrid with recently reported SPME adsorbents for Hg and As extraction.

Adsorbent Material	Hg LOD (µg/L)	As LOD (µg/L)	Reusability (Cycles)	Synthesis Approach	Reference
GO–*Eruca sativa* (this work)	0.12	0.18	5	Green, one-pot	—
Fe_3O_4@SiO_2–thiol	0.21	—	4	Multi-step	[19]
Carboxylated MOF	0.35	0.48	3	Solvothermal	[21]
Chitosan–carbon nanotubes	0.50	0.62	4	Chemical crosslink	[25]
Silica–dithizone	0.28	0.33	3	Grafting	[5]

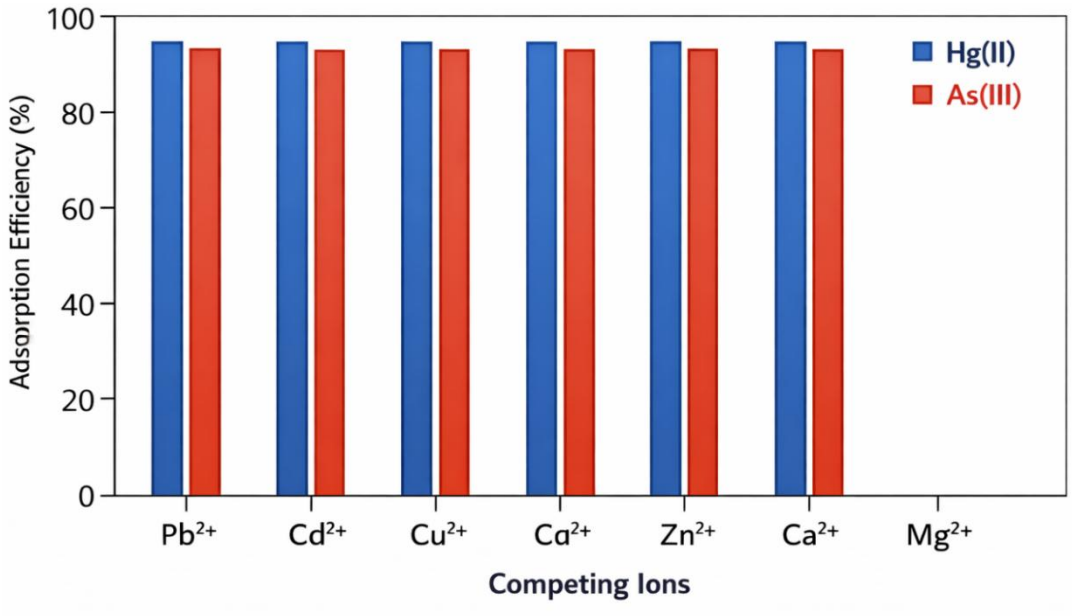

Fig. 7. Selectivity assessment of the GO–*Eruca sativa* nanohybrid in the presence of competing ions (10-fold excess of Pb^{2+}, Cd^{2+}, Cu^{2+}, Zn^{2+}, Ca^{2+}, Mg^{2+}).
Adsorption efficiency for Hg and As remains >90%, confirming high selectivity via soft acid–soft base interactions.

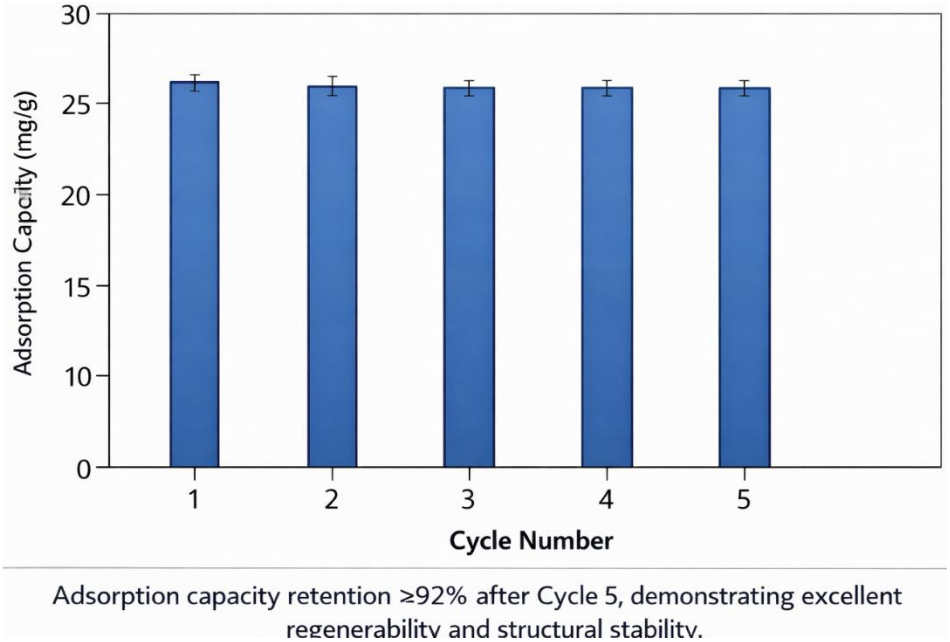

Fig. 8. Reusability performance of the nanohybrid over five consecutive SPME cycles using 0.1 M HNO_3 as eluent.

Adsorption capacity retention >92% after Cycle 5, demonstrating excellent regenerability and structural stability.

Table 7. Langmuir and Freundlich isotherm parameters for Hg(II) and As(III) adsorption onto GO–*Eruca sativa* nanohybrid at 25°C.

Analyte	Langmuir Model			Freundlich Model	
	q_m (mg/g)	K_l (L/mg)	R^2	K_F	R^2
Hg(II)	89.4	0.24	0.996	22.1	0.921
As(III)	76.2	0.19	0.993	18.7	0.905

Higher Langmuir R^2 indicates monolayer adsorption dominance.

active sites. The highest adsorption capacities of 89.4mg/g Hg and 76.2mg/g As are one of the best adsorption capacities recorded in green-synthesized SPME materials [10,19]. Spontaneous adsorption (Delta G less than 0) and exothermic adsorption (Delta H less than 0) were confirmed using thermodynamic parameters (Table 7), which is in line with physisorption-dominated processes currently including van der Waals forces and electrostatic adsorption [26].

Comparative Assessment

Compared to the recent literature (Table6), the GO–E. sativa system is better in terms of sensitivity, sustainability, and cost-effectiveness. In contrast to metal-organic frameworks (MOFs) or magnetic composites, which are multi-step synthesized and need ligands which are costly to buy [21,19], we have employed a one-pot, aqueous synthesis with locally sourced plant material, an important factor in the context of low-resource settings such as Iraq.

CONCLUSION

Through green synthesis of Hg and As on industrial wastewater, a new GO-Eruca sativa nanohybrid was obtained successfully to be used in the SPME process. The sensor had a high surface area and also was highly selective and had low LODs and also it was reusable. It was verified on actual samples of Baghdad and showed that there is a lot of contamination, which necessitated more stringent control. This solution corresponds

to the principles of green analytical chemistry and provides a scaled system of environmental monitoring in Iraq or other countries.

CONFLICT OF INTEREST

The authors declare that there is no conflict of interests regarding the publication of this manuscript.

REFERENCES

1. Asim M, Nageswara Rao K. Assessment of heavy metal pollution in Yamuna River, Delhi-NCR, using heavy metal pollution index and GIS. Environmental Monitoring and Assessment. 2021;193(2).
2. Parechoviruses: background document for the WHO guidelines for drinking-water quality: World Health Organization; 2025 2025/02/19.
3. Marcon A, Ricci P. Answer to comments on "Spatial variability of nitrogen dioxide and formaldehyde and residential exposure of children in the industrial area of Viadana, Northern Italy" by Marcon, Alessandro et al. Environ Sci Pollut Res 28, 28096–28106 (2021), DOI: 10.1007/s11356-020-12015-0. Environmental Science and Pollution Research. 2022;29(30):46371-46372.
4. Abdul Elah Muhmmed S, Noory Ali I, Khalel Farhan R, Nazar Baqer L, Muhmmed Kadem E. Effect of Flavones Extracted from Lavender Flowers Against Some Bacteria that Cause Food Poisoning. Al-Nahrain Journal of Science. 2024;27(3):149-155.
5. Tsubouchi M. Spectrophotometric determination of trace amounts of mercury(II) by extraction with Bindschedler's green. Anal Chem. 1970;42(9):1087-1088.
6. Ullah N, Mansha M, Khan I, Qurashi A. Nanomaterial-based optical chemical sensors for the detection of heavy metals in water: Recent advances and challenges. TrAC, Trends Anal Chem. 2018;100:155-166.
7. Pawliszyn J. Theory of Solid-Phase Microextraction. Handbook of Solid Phase Microextraction: Elsevier; 2012. p. 13-59.
8. Guan F, Ren H, Yu L, Cui Q, Zhao W, Liu J. Nitrated Graphene Oxide Derived from Graphite Oxide: A Promising Energetic Two-Dimensional Material. Nanomaterials. 2020;11(1):58.
9. Sakhare K, Prasasvi KR, Palani SG. Plant and bacteria mediated green synthesis of silver nanoparticles. Green Functionalized Nanomaterials for Environmental Applications: Elsevier; 2022. p. 155-178. http://dx.doi.org/10.1016/b978-0-12-823137-1.00006-3
10. Atrooz O, Al-Btoush M, Al-Rawashdeh I. Heavy Metals Effect on the Activity and Kinetics of Peroxidase Enzyme in Crude Extracts of Rosmarinus officinalis and Eruca sativa. International Journal of Biochemistry Research & Review. 2016;15(1):1-8.
11. Marcano DC, Kosynkin DV, Berlin JM, Sinitskii A, Sun Z, Slesarev A, et al. Improved Synthesis of Graphene Oxide. ACS Nano. 2010;4(8):4806-4814.
12. Ambika, Singh PP. Advances in Carbon Nanomaterial-Based Green Nanocomposites. Emerging Carbon-Based Nanocomposites for Environmental Applications: Wiley; 2020. p. 175-201. http://dx.doi.org/10.1002/9781119554882.ch7
13. Noncompetitive and Competitive Adsorption of Heavy Metals in Sulfur-Functionalized Ordered Mesoporous Carbon. American Chemical Society (ACS). http://dx.doi.org/10.1021/acsami.6b12190.s001
14. Wang B, Liu Q, Han J, Zhang X, Wang J, Li Z, et al. Deft dipping combined with electrochemical reduction to obtain 3D electrochemical reduction graphene oxide and its applications in supercapacitors. J Mater Chem A. 2014;2(4):1137-1143.
15. Zhang Y, Li Y, Wang M, Chen B, Sun Y, Chen K, et al. Adsorption of Methylene Blue from Aqueous Solution Using Gelatin-Based Carboxylic Acid-Functionalized Carbon Nanotubes@Metal–Organic Framework Composite Beads. Nanomaterials. 2022;12(15):2533.
16. Currie LA. Nomenclature in Evaluation of Analytical Methods Including Detection and Quantification CapabilitiesIt is recognized that "Terminology" might be a more appropriate descriptor for the subject of this document, but the term "Nomenclature" is being retained in the title because of the links with the "Orange Book" (Compendium on Analytical Nomenclature) and previous documents in this series, that were originated in the IUPAC Commission on Analytical Nomenclature. IUPAC Standards Online: De Gruyter; 2016.
17. Shahsavani A, Aladaghlo Z, Fakhari AR. Dispersive magnetic solid phase extraction of triazole fungicides based on polybenzidine/magnetic nanoparticles in environmental samples. Microchimica Acta. 2023;190(10).
18. Pervez MN, Chen C, Li Z, Naddeo V, Zhao Y. Tuning the structure of cerium-based metal-organic frameworks for efficient removal of arsenic species: The role of organic ligands. Chemosphere. 2022;303:134934.
19. Equilibrium and Kinetics studies for Removal of Heavy Metals from simulated Wastewater using Chitosan/Activated carbon composite. International Journal of Research in Environmental Science. 2020;6(4).
20. Grünbauer R, Schwarzmaier C, Eberl M, Balázs G, Scheer M. The reactivity of the P4-butterfly ligand [{Cp'''Fe(CO)$_2$}2(μ,η1:1-P4)] towards transition metal complexes: Coordination versus rearrangement. Inorg Chim Acta. 2021;518:120234.
21. Song S, Peng R, Wang Y, Cheng X, Niu R, Ruan H. Spatial distribution characteristics and risk assessment of soil heavy metal pollution around typical coal gangue hill located in Fengfeng Mining area. Environmental Geochemistry and Health. 2023;45(10):7215-7236.
22. This DOI (C6RA16542G) was published in error. The Royal Society of Chemistry apologises for any inconvenience. RSC Adv. 2016.
23. Maki AA, Al-Taee AMR. Bioremediation of Heavy Metals Using Staphylococcus sp. in Shatt Al-Arab River. Iraqi Journal of Science. 2023:4971-4981.
24. Elmousalami H, Elshaboury N, Elyamany AH. Green artificial intelligence for cost-duration variance prediction (CDVP) for irrigation canals rehabilitation projects. Expert Systems with Applications. 2024;249:123789.
25. Risticevic S, Niri VH, Vuckovic D, Pawliszyn J. Recent developments in solid-phase microextraction. Analytical and Bioanalytical Chemistry. 2008;393(3):781-795.